Article

Not peer-reviewed version

Investigation of Texture, Thermal Conduction and Some Mechanical Properties of Melamine Formaldehyde Foam and Melamine Formaldehyde-Organo-Clay Nanocomposite and Some Hybrid Composites

Ahmet Gürses * and Elif Şahin

Posted Date: 7 September 2023

doi: 10.20944/preprints202309.0423.v1

Keywords: Mineral filled composites; Nano composite; Organo clay; Melamine formaldehyde, Thermal insulation, Mechanical strength, Hybrid composites

Article

Investigation of Texture, Thermal Conduction and Some Mechanical Properties of Melamine Formaldehyde Foam and Melamine Formaldehyde-Organo-Clay Nanocomposite and Some Hybrid Composites

Ahmet Gürses [1,*] and Elif Şahin [2]

[1] Atatürk University, K.K. Education Faculty, Department of Chemistry Education, Erzurum, Turkey ahmetgu@yaoo.com; agurses@atauni.edu.tr

[2] Atatürk University, Nanoscience and Nano Engineering Department, Erzurum, Turkey, sahine@atauni.edu.tr

* Correspondence: ahmetgu@yahoo.com; agurses@atauni.edu.tr,+904422314004

Abstract: Generally, mineral fillers are added to thermoplastic polymers to reduce cost and improve performance. However, properly selected mineral fillers can also improve thermal conductivity and deformation behavior, shrinkage, impact strength, dimensional stability, and molding cycle time in thermoset polymers. This study focused on the preparation and microscopic and spectroscopic characterization of various hybrid composites using pumice as primary filler and gypsum, kaolin and hollow glass sphere as secondary fillers, as well as examining some of their mechanical properties and thermal conductivities. For this, first of all, surface modification of the clay was carried out by intercalation method from solution using raw Montmorillonite, cationic surfactant and long chain hydrocarbon material, and then organo-clay melamine formaldehyde nanocomposite was prepared by in situ synthesis using organo clay and melamine formaldehyde pre-polymer. Finally, non-ionic surfactant, foaming agent and glycerin were added to the prepared nano-composite at approximately 90°C, mixed mechanically and then pumice was added. The processes at this stage were repeated while preparing hybrid composites with pumice and other mineral additives. For curing and molding, the composite was first subjected to microwave irradiation for 5 minutes followed by thermal treatment at 140°C for 60 min. Fourier transform infrared spectroscopy (FTIR), X-ray powder diffraction (XRD) spectra and Scanning electron microscope (SEM) and High resolution transmission electron microscope (HRTEM) images were taken for morphological and textural characterization for raw clay (MMT), organo clay (OMMT) and pure polymer with prepared hybrid composites. In addition, some mechanical properties such as bending strength, elasticity modulus and screw holding resistance, as well as thermal conductivity coefficients of the hybrid composites were determined according to the relevant standards and the obtained results were evaluated. Spectroscopic and microscopic analyzes have shown that effective adhesion interactions occur between polymer-clay nanocomposite particles and filler grains, thus resulting in textural arrangements with different properties. Mechanical and thermal conductivity test results showed that melamine formaldehyde-organo-clay nano composite foam and hybrid composite containing hollow glass sphere are highly qualified materials in terms of thermal insulation and mechanical strength.

Keywords: mineral filled composites; nano composite; organo clay; melamine formaldehyde; thermal insulation; mechanical strength; hybrid composites

 doi:10.20944/preprints202309.0423.v1

1. Introduction

The development of new generation adhesives with better properties through nano-technological applications has created a new and great opportunity for the worldwide composite industry. The inclusion of melamine formaldehyde resins in nano-technological applications with nanomaterial reinforcement has enabled the preparation of new highly effective composites that can be used in many industrial areas[1–3]. Micro or nano fillers, which can be organic or inorganic, can improve the mechanical properties, electrical and thermal conductivity, thermal behavior and fire retardant properties of melamine formaldehyde resin. For this, formulations using various nanomaterials and additives such as carbon nanofibers, nano cellulose, nano clay, nano-SiO_2, nano-TiO_2, zinc oxide and alumina have been developed [4–7]. Thermoset polymers with lower curing shrinkage and higher dimensional stability are widely used matrix materials due to their high tensile strength and modulus of elasticity and high adhesion properties [8]. Many hardening agents such as spherical rubber particles, liquid rubbers, glass beads, and branched polymers are often used to increase the ductility of thermoset polymers, but they can adversely alter properties such as glass transition temperature (T_g), tensile strength, and modulus of elasticity [9]. Nanoparticles, which can generally improve the mechanical and viscoelastic properties of composites, may also tend to agglomerate due to their high surface areas and attractive interactions [10]. For this reason, the degree of dispersion and homogeneity of the nanoparticles in the resin are of critical importance in order to ensure an effective interaction between the matrix and the nanoparticles and to obtain maximum benefit from the high surface areas[11,12].

In particular, uniform dispersion of nanoparticles in the matrix is extremely important in terms of increasing toughness and obtaining other desired material properties [13,14]. Due to the relatively low cost and prevalence, the use of modified clays as nanofillers is becoming increasingly common. The addition of nano-clay to the polymer matrix can improve thermal degradation resistance, barrier properties and mechanical strength [15–18]. The improvement in mechanical properties is mainly attributed to the excellent particle-particle and particle-matrix interaction in the nanocomposite and the high aspect ratio of the nano-filler [19]. Mineral and fiber-filled polymer nanocomposites have attracted great attention in research as well as in industry, as they can exhibit improved properties and can be easily processed [20]. The improvement of mechanical properties of composites depends mainly on the type of polymer, fiber and filler and preparation technique [20,21]. However, incompatibility between filler and matrix in terms of interfacial properties can have adverse effects on the final properties of the composite, and nanoparticles may need to be incorporated into mineral filled composites to overcome the incompatibility and prepare hybrid composites. The incorporation of nanoparticles can also improve the mechanical properties without causing a significant increase in the weight of the composite [22]. Among the various nanoparticles, organo-clay and especially Montmorillonite (MMT) and its modified form, organo Montmorillonite (OMMT), have emerged as a very suitable alternative for polymeric composites [23–27]. Composite materials are heterogeneous materials with wide application areas such as construction, aviation, automotive, thermal conductivity, electrical and thermal insulation and packaging [28–30]. Due to critical factors such as low density and cost, polymer matrix composites have become increasingly popular, especially in the automotive and aerospace fields. Composites, which have unique advantages that their components cannot meet, are developed to produce changes according to certain requirements without changing the basic functions of the materials. According to their main matrices, composites are divided into three types as metal, ceramic and polymer matrix. The polymer matrix is also classified as thermoplastic and thermoset plastic matrices, and thermoset polymers have some advantages over thermoplastics such as ease of manufacture, faster curing, flame retardancy, protection of structural integrity against heating. Many reinforcements can be added to the matrix to improve the properties of brittle thermoset resins. The reinforcements can be long and short fibers, particles, flakes, and the particles can have various geometries, including layered, spherical, tubular, randomly shaped, and the particle sizes can also vary from a few nanometers to a few 100 μm [28,30–32]. Thermosets and thermoplastics are two polymer groups used as matrix materials in polymer matrix composites (PMC). Nylon, cellulose acetate, polystyrene, polypropylene, polyethylene,

 doi:10.20944/preprints202309.0423.v1

polycarbonate, polyvinyl chloride, polyether-ether ketone and acrylonitrile-butadiene-styrene are generally used as thermoplastic matrices, phenolic, epoxy, polyester, polyimide and polyurethane resins are used as thermoset matrices [33]. The most important advantage of thermoset matrices is ease of processing and this encourages their use in critical industries. However, the most obvious disadvantages are that they cannot be used to obtain other shapes after curing and that they require high temperature and pressure for molding. Ease of manufacture of thermoset composites [34,35]. Generally, polymer matrix composites in which thermoset polymers are used as matrix and at least two different components as additives are called hybrid polymer matrix composites (HPMC). The use of two different components can give HPMC some superior properties that cannot be achieved with a single component [36]. Hybrid polymer composites play an important role in structural applications due to their multidimensional performance [37].

Polymers that need to be modified to improve both their mechanical and tribological performance can be modified through polymer blending, copolymerization, and reinforcing fillers and/or fibers. It is also known that polymer blending is the most effective method for polymer modification and the addition of fillers and fibers effectively increases the strength of polymer and polymer composites [38]. In addition to micro-fillers, which alone can play an important role in improving the behavior of polymer composites, some nano-fillers such as titanium dioxide (TiO_2), clay, molybdenum disulfide (MoS_2), silicon carbide (SiC) and alumina also have the potential to improve the mechanical behavior of polymer nanocomposites [37,39]. However, excessive addition of nanoparticles can also reduce the strength of hybrid composites. Fillers, which are primarily used in resin-based composites to reduce production costs, can also improve the mechanical and thermal properties of the composite, and granular mineral fillers can exhibit effects such as increasing the hardness of the matrix, reducing the coefficients of thermal expansion and reducing volume shrinkage during curing. Reduction of thermal expansion and cure shrinkage is very important in laminated composite structures [40,41]. Polymer composites generally consist of at least two phases, one with a polymer as the matrix and the other with a continuous or discontinuous filler or reinforcement such as whiskers, particles, and fibers.[42].

Although there are many types of fillers today, mineral-based fillers such as Kaolin, silica, talc and calcium carbonate are used more because they are cheap and abundant in nature. Organo or nano clay, which is prepared with the modification of Montmorillonite (MMT), has been used for a long time as a filler or nano filler in polymer composites. It has been reported that the use of 5% MMT as a filler can improve the mechanical and thermal barrier properties of Nylon 6, and similarly, the addition of nano calcium carbonate and nano clay to high density polyethylene (HDPE) can significantly increase the modulus of elasticity [43,44]. Also, dolomite as filler was able to improve the mechanical and thermal properties of various polymeric materials [45–47]. Fillers can be present in a variety of composite systems commonly used in the packaging, biomedical, cosmetic, pharmaceutical, paper, food, paint and adhesive industries, as they can improve the specific properties of materials such as hardness, durability, clarity, creep resistance. and physical appearance [48]. Since the heterogeneous distribution of a filler in the polymeric matrix may result in the formation of low-performance polymer composites, the desired properties of the polymer composite to be prepared depend on the effective polymer-filler interaction and the homogeneous distribution of the filler. Fillers, which can be particulate or fibrous, may have their own unique properties and advantages, but modifications or the use of extra adapters may be necessary to meet certain requirements and improve their properties and make them more suitable for particular applications. The high aspect ratio of fibrous fillers such as glass fiber and natural fiber can be effective in increasing the strength and stiffness of polymers. Similarly, particulate fillers such as mineral fillers, usually in powder form and in various shapes and sizes, can effectively increase the strength and toughness of polymer matrices. In particular, the size of the filler has a decisive influence on the properties of the polymer composite, and smaller sized fillers with a larger surface area are more preferred for more effective interactions between the filler and the polymer matrix. In addition, ultrafine or nano-sized fillers are used because of their homogeneous dispersion throughout polymeric matrices and their high dispersion efficiency, as well as their ability to prevent possible

 doi:10.20944/preprints202309.0423.v1

filler aggregation at high loading [49]. On the other hand, compatibility between the filler and the polymer matrix is extremely important, as the high interfacial energy caused by the different surface properties of the filler and polymer molecules can lead to the formation of a low-performance inhomogeneous polymer composite. In addition to chemically or physically modifying the filler to produce a homogeneous polymer composite, the use of effective compatibilizers at the matrix and filler interface and the blending technique can also be considered as alternative ways of improvement [48,49]. Since the crosslinking density, which causes the brittle structure and low toughness of thermoset type formaldehyde resins, limits their applications, many studies are carried out to improve the properties of formaldehyde resins such as cracking resistance, dynamic mechanical and thermal stability by adding different types and amounts of nano fillers [47,50–52]. The homogeneous dispersion and breakage of possible nanoclusters in the polymer matrix are the main challenges in the preparation of nanocomposites [53]. The distribution of the cluster size and the dispersion of the nano films in the polymer matrix, the strong interfacial interactions between the fillers and the molecular chains are decisive in changing the basic properties of the pure polymer [54,55]. Studies have intensified to find suitable processing techniques to reduce the tendency of particles to agglomerate and non-homogeneously disperse in the polymer matrix through van der Waals interactions and to ensure effective dispersion. Various techniques such as solution combination, melt intercalation, mechanical blending [56–58] and ultrasonic irradiation [59–61] are commonly used in composite preparation. Nitrogen-rich and stable Melamine formaldehyde resin, which has a triazine ring structure, has superior properties such as thermal stability, fire retardancy, low thermal conductivity, low emission, waterproof, transparency, non-melting. It is widely used in a wide variety of industrial applications such as automotive and automotive. While urea-formaldehyde and epoxy-based nano-composites are frequently studied in scientific and industrial research, studies on melamine formaldehyde resin are not very common [50]. Therefore, this study focused on the preparation of hybrid composites using organo-clay melamine formaldehyde nanocomposite as matrix/adhesive, pumice as primary filler and gypsum, kaolin and hollow glass sphere as secondary fillers and examining their morphological and textural properties. For this purpose, some mechanical tests such as flexural strength, modulus of elasticity, screw holding resistance and thermal conductivity measurements were performed on the composites prepared and the results obtained were evaluated comparatively.

2. Materials and Methods

2.1. Material

In this study, powder pumice used as primary filler to prepare hybrid nanocomposites was obtained from Blokbims Company in Nevşehir, Turkey, and its mineralogical composition is given in Table 1. Kaolin clay which was purchased from Bursa Lazoğlu Co. and its mineral composition is given in Table 2, commercial gypsum plaster, hollow micro glass spheres (HMGS, diameters 100-800 micrometers) were used as secondary filler at 12.5% by weight. In addition, Montmorillonite clay (MMT), which was obtained from Karakayalar Co. in Çankırı, Turkey, and its mineralogy composition is given in Table 3, was used to prepare organo Montmorillonite (OMMT) to be used as nano filler.

Preprints (www.preprints.org) | NOT PEER-REVIEWED | Posted: 7 September 2023 doi:10.20944/preprints202309.0423.v1

Table 1. The mineralogical composition of the pumice.

Component (%)											
SiO_2	Al_2O_3	CaO	MgO	Fe_2O_3	K_2O	Na_2O	TiO_2	MnO	SrO	SO_3	Other
73.35	12.88	0.77	0.08	1.10	4.40	3.82	0.08	0.05	0.01	0.44	3.02

Table 2. Mineralogical content of Kaolin.

Components (%)									
SiO_2	Al_2O_3	Fe_2O_3	MgO	CaO	Na_2O	K_2O	TiO_2	Cr_2O_3	Other
71.00	20.00	0.40	0.05	0.15	0.10	0.35	0.50	0.02	7.93

Table 3. Mineralogical content of Montmorillonite.

Components (%)									
SiO_2	Al_2O_3	Fe_2O_3	MgO	CaO	Na_2O	K_2O	TiO_2	SO_3	Other
59.32	17.19	5.95	3.63	2.21	1.68	0.97	0.74	0.51	7.81

For the synthesis of Melamine Formaldehyde resin to be used as the composite matrix, Melamine and Formaldehyde (37%), as well as the nonionic surfactant used for encapsulation, Tween 80, and Glycerin are of analytical grade were obtained from Merck Co. and also gasoline, which is a mixture of isooctane, butane and 3-ethyltoluene, supplied from the gas station.

2.2. Method

2.2.1. Preparation of organo clay

Organo clay (OMMT) to be used as nano filler was prepared by solution intercalation method using a cationic surfactant, Cetyltrimethyl ammonium Bromide, CTAB (purchased from Merck Co.), hydrocarbon material (Table 4) and Montmorillonite clay (Table 2). For this, firstly, an aqueous solution of CTAB was prepared at 40oC by adding the amount of CTAB corresponding to the concentration of 160mg/L, and then hydrocarbon material was added at a ratio of 0.3 g/1.0 g. After the resulting dispersion was mixed mechanically for 30 minutes at a mixing speed of 50 min-1, sufficient amount of raw Montmorillonite (MMT) was added to the hydrocarbon-water dispersion and mixing was continued for 30 minutes at a mixing speed of 200 min-1. Finally, the mixture was filtered and dried at 110°C for 2 hours, ground and sieved in ASTM standard 200 mesh and stored in a sealed container for further experiments [62,63].

Table 4. Some characteristics of hydrocarbon material.

Density (15 ^{0}C), kg/m^3	Calorific value MJ/kg	Flash point ^{0}C	Water by distillation, wt. %	C	H	N	S	Ash
990.7	42.74	105.8	0.1	83.4	11.9	0.8	1.5	0.03

2.2.2. Preparation of melamine formaldehyde pre polymer (MF) and hybrid composites

At a ratio of 1.0/1.1, melamine and 37 % wt. formaldehyde were placed in a three-necked flat bottom flask with magnetic stirring thermometer and cooling equipment and heated at approximately 60oC for a certain period of time until the solution became clear. Then, the pH was adjusted to 8.5 with 40% wt. NaOH solution and refluxed for 1 h at approximately 95oC considering the viscosity of the mixture. Then, a sufficient amount of concentrated acetic acid for neutralization,1.0% by weight of Glycerin and Tween 80, as well as 6.0% by weight of gasoline were added to the resulting pre polymer, and vigorously mixed mechanically to ensure a homogeneous mixture. Mixing was continued by adding a certain amount of pumice and other fillers. The foaming method was used for the encapsulation and for this, the resulting mixture was exposed to microwave

 doi:10.20944/preprints202309.0423.v1

radiation for 2 min in a microwave oven in a suitable container. Finally, it was taken into a modular square aluminum mold with an internal volume of 10x10x1 cm3, and the mixture was thermally treated for 1 h at 140 °C in a hot air heated oven to remove water, residual formaldehyde as well as complete curing [64].

For the characterization of pure MF resin, raw fillers and composites, Fourier transform infrared spectroscopy (FTIR), X-ray powder diffraction spectroscopy (XRD), Scanning electron microscopy (SEM) High resolution transmittance electron microscopy (HRTEM) analyzes as well as mechanical tests such as bending, elasticity modulus, compressive strength and screw withdrawal resistance and thermal conductivity coefficient measurements were performed [65].

2.2.3. Fourier transform infrared spectroscopy (FTIR) analysis

FTIR spectra of raw clay, organo clay, mineral fillers and hybrid composites were taken to determine their functional groups using taken using Vertex 70 V FTIR spectrometer in the range of 4000 to 400 cm-1 with an average of 100 scans and 1 cm-1 resolution.

2.2.4. X-ray powder diffraction spectroscopy (XRD) analysis

In layered clays such as montmorillonite, the variation of the interlayer spacing is taken into account to determine the type of composite prepared [66]. In order to examine the deformations in the crystal structures of the components, XRD diffractograms of hybrid composites prepared using mineral fillers with varying ratios with fixed organo clay ratio were taken using a PANalytical Empyrean X-ray Difractometer with Cu Ka1 (1.540 Å) radiation operating at 5 kV and 40 mA in the range of 2θ 9-90◦ and at the scanning speed of 4/min.

2.2.5. Scanning electron microscopy (SEM) analysis

In order to observe and evaluate the morphological changes that may occur in the composites due to adhesion interactions between organo clay, polymer matrix and mineral fillers and the polymer matrix and encapsulated particles, SEM images of raw clay, mineral fillers and composites were taken using a Scanning Electron Microscope (SEM) (FEI-INSPECT S50 model) at 30 kV.

2.2.6. High resolution transmittance electron microscopy (HRTEM) analysis

HRTEM analysis is of great importance in examining the textural structures of materials at the nanoscale, and especially the distribution of nanoparticles in nanocomposites [67]. In this study, HRTEM images of raw clay, organo clay, mineral fillers and hybrid composites were taken to characterize their textural structures using a HITACHI HT7700 high resolution transmission electron microscope (LaB6 filament) operating at 120.0 kV.

2.2.7. Mechanical tests and thermal conductivity measurements

Direct screw withdrawal - screw holding tests and bending (bending and modulus of elasticity) tests of pure MF foam, MF-organo clay nano-composite and hybrid composites were performed using a universal testing machine (Zwick/Roell) according to ASTM 1037-16 [68] and ASTM D790 [69] standards, respectively. The thermal conductivity coefficients of pure MF foam, MF-organo clay nano-composite and hybrid composites were also measured using a thermal conductivity meter with probe consisting of a single heater wire and thermocouple. (Quick Thermal Conductivity Meter QTM-500, Japan).

The codes and component ratios corresponding to pure MF, MF-organo clay nanocomposite, and MF- organo clay-pumice-gypsum, MF- organo clay-kaolin and MF- organo clay-hallow glass sphere hybrid composites are given in Table 5.

Preprints (www.preprints.org) | NOT PEER-REVIEWED | Posted: 7 September 2023 doi:10.20944/preprints202309.0423.v1

Table 5. Codes and component ratios of pure MF, MF-organo clay nanocomposite, and MF- organo clay-pumice, MF- organo clay-pumice-gypsum, MF- organo clay-kaolin and MF- organo clay-hallow glass sphere hybrid composites.

Specimen code	Nano filler (Organo clay) (%wt.)	Primary filler (%wt.)		Secondary filler (%wt.)	
MF	-	-	-	-	
MFCNC	0.11	-	-	-	
MFCPHC	0.11	Pumice	44.4		-
MFCPGHC	0.11	Pumice	38.9	Gypsum	5.5
MFCPKHC	0.11	Pumice	38.9	Kaolin	5.5
MFCPHHC	0.11	Pumice	38.9	Hallow glass sphere	5.5

3. Results

3.1. Textural characterization of raw montmorillonite (MMT), organo-montmorillonite (OMMT), melamine formaldehyde resin (MF), melamine formaldehyde orgono clay nanocomposite (MFCNC) and hybrid composites

In order to compare the differences in the textural structures of raw montmorillonite (MMT), organo montmorillonite (OMMT) and raw pumice and to see the effectiveness of the modification made for lyophilization, HRTEM images of both were taken and are given in Figure 1 a and b, respectively. Dark long fibrous lines appearing in HRTEM images indicate clay grains with their 2:1 layered structure.

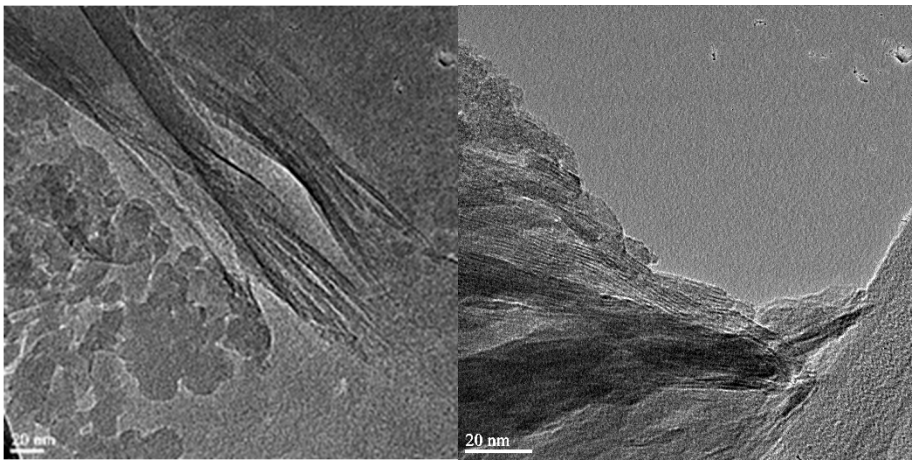

(a) (b)

Figure 1. HRTEM images of raw montmorillonite (MMT) (a) and organo montmorillonite (OMMT) (b).

From Figure 2a it can be seen that pure melamine formaldehyde resin forms as aggregated microspheres and aggregates develop in three dimensions [70]. This textural arrangement is due to the use of the microwave irradiation assisted foaming method before curing. Figure 2b shows that the MF molecule clusters become regularly sparse or disaggregated, preserving their spherical structure, due to the exfoliation of the organo clay platelets into the polymer matrix [71]. The HRTEM image of the MF-organo clay-pumice composite (MFCPHC) in Figure 2c shows that the pumice has a vesicular coarse-textured and glassy structure, but the particles are effectively surrounded by spherical polymer clay nanocomposites [72]. From the HRTM image of the MF-organo clay-pumice-gypsum hybrid composite (MFCPGHC) in Figure 2d, it can be seen that relatively regular gypsum plates are heterogeneously dispersed next to the pumice plates with a glassy structure, and the particles are surrounded by distinctly deformed polymer clay nanocomposite spheres [73]. On the

 doi:10.20944/preprints202309.0423.v1

other hand, in the image of the MF-organo clay-kaolin hybrid composite (MFCPKHC) in Figure 2e, it can be seen that coarse textured glassy pumice plates, spherical polymer clay nanocomposites and kaolin plates can exhibit an effective blending [74]. The HRTM image of the MF-organo clay-hollow glass sphere hybrid composite (MFCPHHC) in Figure 2f shows that the pumice plates exhibit a more regular and relatively uniform arrangement with the inclusion of hollow glass spheres encapsulated by spherical polymer clay nanocomposites [75].

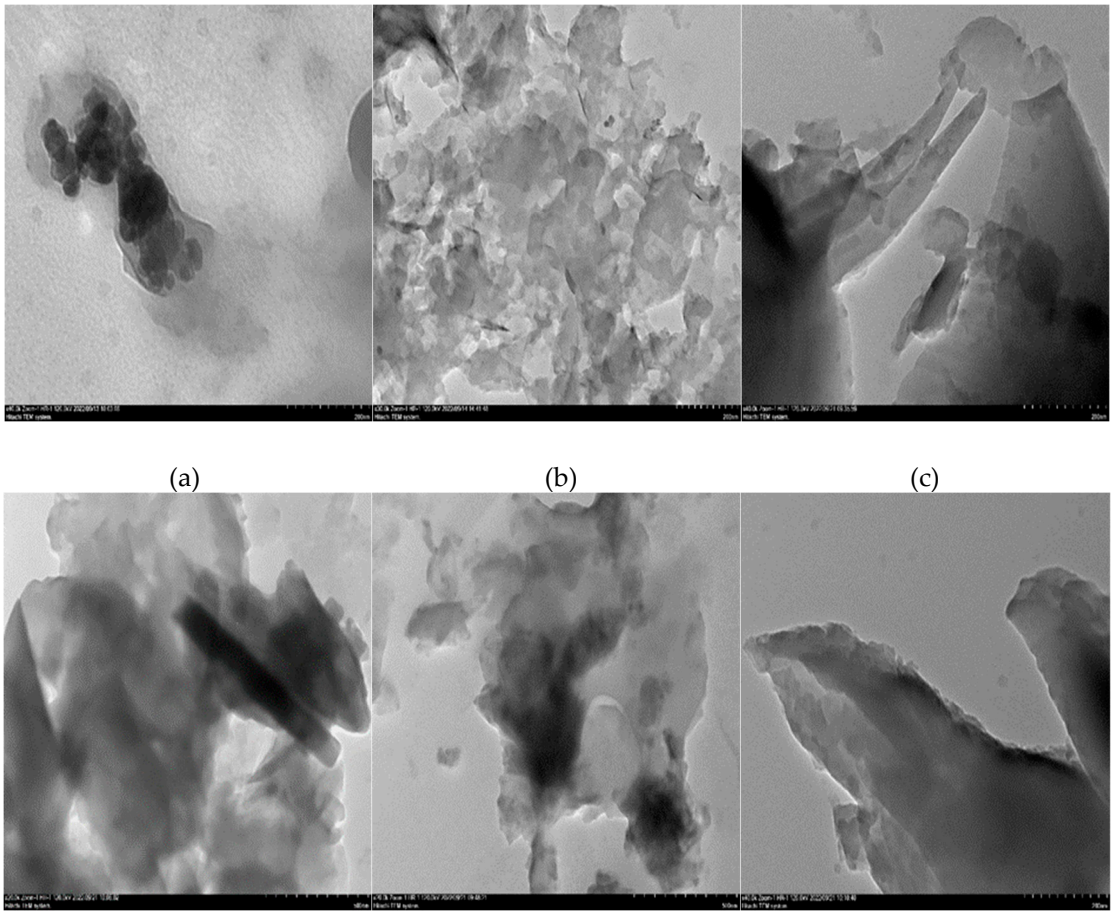

(a) (b) (c)

(d) (e) (f)

Figure 2. HRTEM images of pure melamine formaldehyde resin (MF) (a), MF-organo clay nanocomposite (MFCNC)(b), and MF- organo clay-pumice (MFCPHC)(c), MF- organo clay-pumice-gypsum (MFCPGHC)(d), MF- organo clay-pumice-kaolin (MFCPKHC)(e) and MF- organo clay-pumice-hallow glass sphere (MFCPHHC) (f) hybrid composites.

3.2. Surface morphological characterization of melamine formaldehyde resin (MF), melamine formaldehyde orgono clay nanocomposite (MFCNC) and hybrid composites

SEM patterns taken for pure melamine formaldehyde resin (MF), MF-organo clay nanocomposite (MFCNC) and MF- organo clay-pumice (MFCPHC), MF- organo clay-pumice-gypsum (MFCPGHC), MF- organo clay-pumice-kaolin (MFCPKHC) and MF-organo clay-pumice-hollow glass sphere (MFCPPHHC) hybrid composites are given in Figure 3.

It can be seen from Figure 3a that the pattern of pure melamine formaldehyde resin clearly reflects the surface morphology showing that clusters of microspheres develop as branched structures in three dimensions [76,77]. Figure 3b reveals a surface morphology showing the ordered stacking of MF molecule clusters in which the branched structure almost disappears, preserving their spherical structure due to the exfoliation of the organo clay platelets into the polymer matrix.

Preprints (www.preprints.org) | NOT PEER-REVIEWED | Posted: 7 September 2023 doi:10.20944/preprints202309.0423.v1

In the SEM pattern of the MF-organo clay-pumice composite (MFCPHC) in Figure 3c, it is seen that the pumice with vesicular coarse texture and glassy structure exhibits a surface morphology covered with spherical polymer clay nanocomposites, including its micro cavities [78,79].

The SEM pattern of the MF-organo-clay-pumice-gypsum hybrid composite (MFCPGHC) in Figure 3d shows the morphological structure implying a regular coating formed by polymer clay nanocomposite spheres in the cavities in the porous pumice plates and superficial fold or fractures. It can be seen again from this figure that a rough surface appearance appears indicating the presence of heterogeneous agglomerates in size. It can be argued that this appearance is related to the presence of glassy pumice plates, gypsum plate fractures and stacked forms of them, surrounded by polymer clay nanocomposite spheres [80].

The image of the MF-organo clay-kaolin hybrid composite (MFCPKHC) in Figure 3e shows that the coarse-textured glassy pumice plates exhibit a surface morphology that indicates a fairly uniform association of spherical polymer clay nanocomposites with kaolin layers arranged in different directions but regularly. On the other hand, Figure 3f shows a surface morphology in which an ordered and relatively localized arrangement of hollow glass spheres clustered together and spherical polymer clay nanocomposites neatly surrounded by pumice plates and kaolin layers appears [81,82].

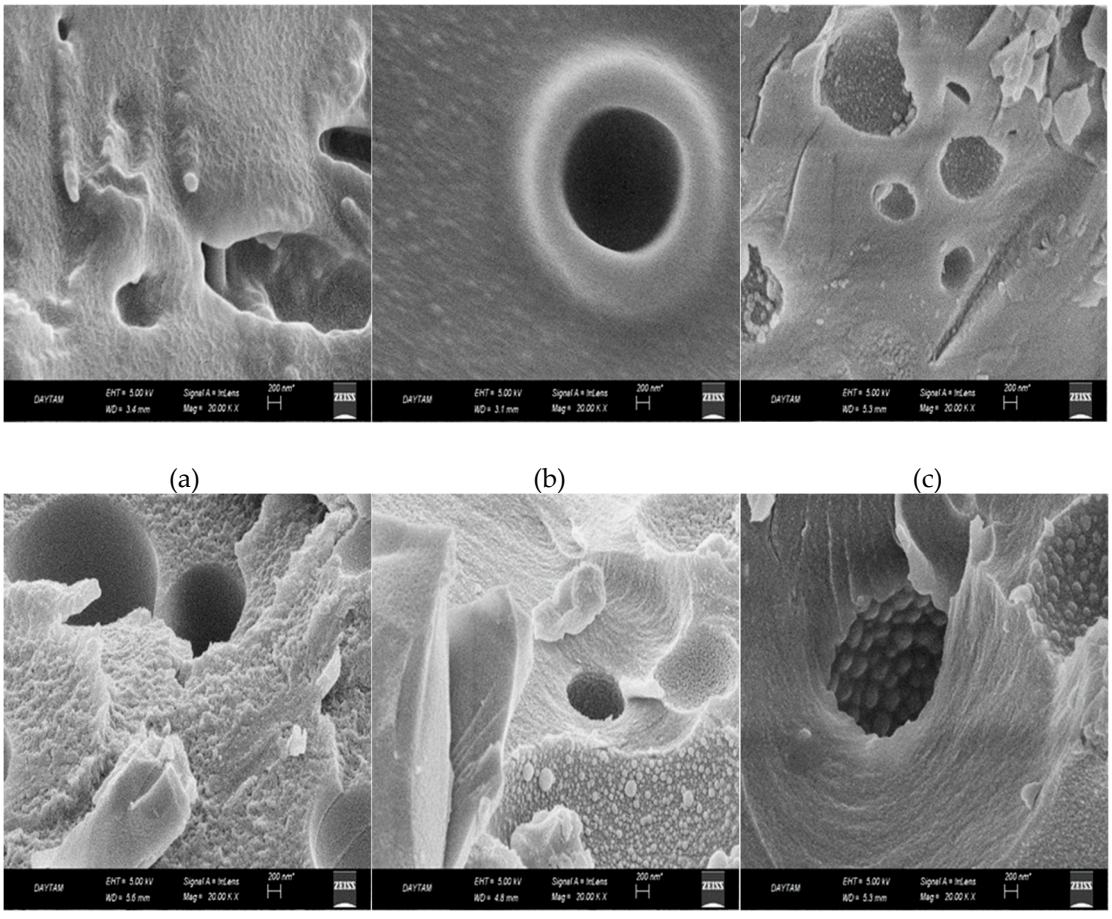

(a) (b) (c)

(d) (e) (f)

Figure 3. SEM patterns of pure melamine formaldehyde resin (MF) (a), MF-organo-clay nanocomposite (MFCNC)(b), and MF- organo-clay-pumice (MFCPHC)(c), MF- organo-clay-pumice-gypsum (MFCPGHC)(d), MF- organo-clay-pumice-kaolin (MFCPKHC)(e) and MF- organo-clay-pumice-hallow glass sphere (MFCPHHC) (f) hybrid composites.

Preprints (www.preprints.org) | NOT PEER-REVIEWED | Posted: 7 September 2023 doi:10.20944/preprints202309.0423.v1

3.3. Analysis of FT-IR Spectra of raw montmorillonite (MMT), organo-montmorillonite (OMMT), melamine formaldehyde resin (MF), melamine formaldehyde organo-clay nanocomposite (MFCNC) and hybrid composites

FT-IR spectra of pure melamine formaldehyde resin (MF), MF-organo clay nanocomposite (MFCNC) and MF-organo-clay-pumice (MFCPHC), MF-organo-clay-pumice-gypsum (MFCPGHC), MF-organo-clay-pumice-kaolin (MFCPKHC) and MF-organo-clay-pumice-hollow glass sphere (MFCPHHC) hybrid composites are given in Figure 4.

The peaks at 3327 cm^{-1}, 1016 cm^{-1}, 1541 cm^{-1} and 1450 cm^{-1} in the FTIR spectrum of MF in Figure 4a correspond to the stretch vibration of N-H and O-H bonds, the stretch vibration of C-O-C bonds and the stretch vibration of C=N, respectively. Accordingly, it can be said that melamine formaldehyde resin was successfully synthesized [83].

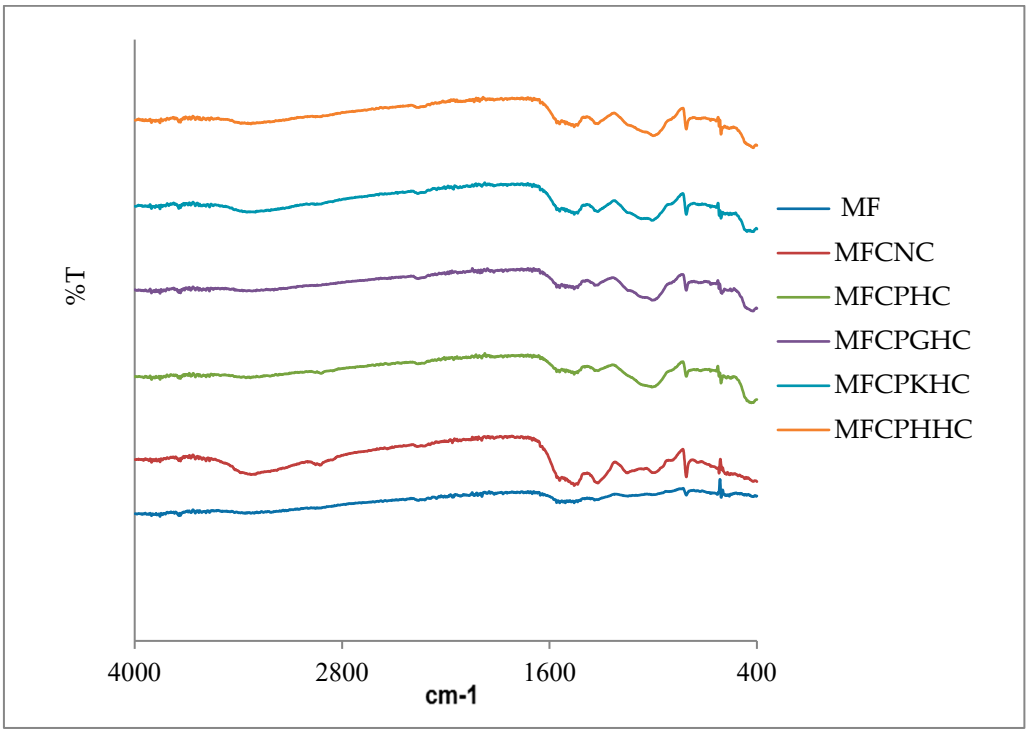

Figure 4. FT-IR spectra of pure melamine formaldehyde resin, MF-organo-clay nanocomposite and various hybrid composites.

In Figure 4, in the FT-IR spectrum of MF-organo-clay nanocomposite (MFCNC), apart from the strong peak at 3354 cm^{-1} from CTAB, three more peaks appeared at 2926, 2914 and 2881 cm^{-1}, corresponding to secondary amine group stretching C–H anti-stretching and C–H stretching. All these specific peaks appeared both at lower density and shifted to lower values due to interactions between clay layers and CTA^+ ions bound by long chain hydrocarbon molecules. Also, two peaks were observed at 1454 cm^{-1} and 1129 cm^{-1}, respectively, corresponding to C–N stretching and N–H bending of CTAB. On the other hand, it can be claimed that the peaks appearing in the 1302-1657 cm^{-1} region are due to the CH2 shear vibration mode and the O-H bending mode of the water molecule around the bound head group. Si-O and Al-OH are the main functional groups observed in the range of 1000 cm^{-1} to 500 cm^{-1}. While the peak at 866 cm^{-1} corresponds to Al-OH bending vibrations, the double Si-O-Si bonds in SiO2 at 802 cm^{-1} and Si-O stretching vibrations observed around 714-617 cm^{-1} indicate the presence of quartz. Strong bands around 3356-3730 cm^{-1} indicate the presence of hydroxyl bonds. The appearance of these peaks as low intensity and shifted from their specific values may also indicate intense interactions between clay plates and long chain hydrocarbon-bound CTA^+ ions [84,85].

Preprints (www.preprints.org) | NOT PEER-REVIEWED | Posted: 7 September 2023 doi:10.20944/preprints202309.0423.v1

In the FT-IR spectrum of the MF-organo clay-pumice composite (MFCPHC) in Figure 4, besides the characteristic peaks of organo-clay and MF origin, slightly shifted and low-intensity peaks corresponding to Al-OH bending vibrations and Si-O stretching vibrations appeared at 905 and 757-635 $cm^{-1.}$ Similar to the other spectra, the peak around 3761 cm^{-1} indicates the presence of hydroxyl groups originating from water [79,86]. The lower peak intensities and shifts can be attributed to the effective interactions between pumice plates and organo clay layers, as implied by the HRTEM images of this hybrid composite.

The FT-IR spectrum of the MF-organo clay-pumice-gypsum hybrid composite (MFCPGHC) in Figure 4 shows a very close similarity to the spectrum of the composite containing only pumice. This is in line with the HRTEM image, which shows that relatively regular gypsum plates are heterogeneously dispersed next to the pumice plates and the particles are surrounded by deformed polymer clay nanocomposite spheres. However, it can be seen that the spectrum also includes the peaks at 663 and 598 cm^{-1}, which correspond to the stretching and bending modes of the sulfate group and other low-intensity characteristic peaks at 1022 and 2337 cm^{-1}.

On the other hand, the FT-IR spectra of the MF-organo-clay-pumice-kaolin (MFCPKHC) and MF-organo-clay-pumice-hollow glass sphere (MFCPHHC) hybrid composites in Figure 4 seem to be quite similar. In terms of the nature of interactions, this is consistent with the fact that the pumice plates, spherical polymer clay nanocomposites and kaolin plates exhibit an efficient blending, and the pumice plates show a more regular and relatively uniform arrangement with the inclusion of hollow glass spheres encapsulated by the spherical polymer clay nanocomposites (see Figure 3e and f). However, it can be argued that low intensity but characteristic peaks at 3759, 3639, 3580 and 3578 cm^{-1} indicate the regular structure of kaolinite. The peaks at 1112 cm^{-1}, 1074 cm^{-1} and 1016 cm^{-1} in the spectrum of the kaolinite-containing composite are Si-O stretching modes, and the peaks at 1112 and 1016 cm^{-1} correspond to the symmetric and anti-symmetric stretching of Si-O bonds. The peak around 418 cm-1 and the peak around 3435 cm^{-1} and the low intensity peak around 1632 cm^{-1} appearing in the spectra of both composites can be attributed to an O-Al-O bending and an OH bending, respectively [81,82,87–89].

3.4. Characterization of mineralogical structures of raw montmorillonite (MMT), organo-montmorillonite (OMMT), melamine formaldehyde resin (MF), melamine formaldehyde orgono-clay nanocomposite (MFCNC) and hybrid composites

Figure 5 shows XRD diffractograms of pure melamine formaldehyde resin (MF), MF-organo clay nanocomposite (MFCNC) and the hybrid composites such as MF-organo-clay-pumice (MFCPHC), MF-organo-clay-pumice-gypsum (MFCPGHC), MF-organo-clay-pumice-kaolin (MFCPKHC) and MF-organo-clay-pumice-hollow glass sphere (MFCPHHC).

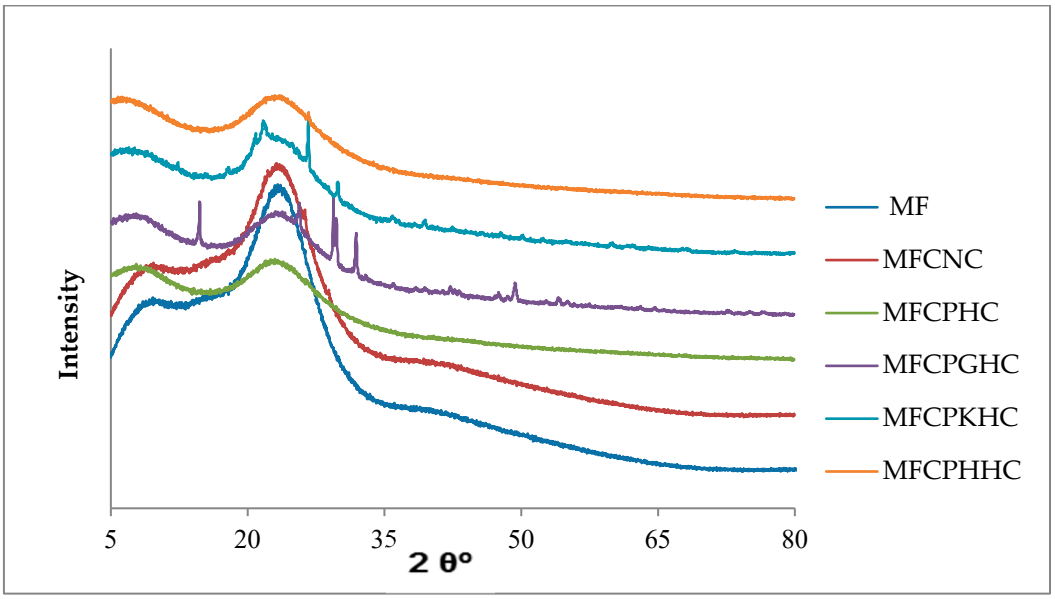

 doi:10.20944/preprints202309.0423.v1

Figure 5. XRD diffractograms of pure melamine formaldehyde resin, MF-organo-clay nanocomposite and various hybrid composites.

Figure 5 shows that in the XRD pattern of the MF resin, two typical broad peaks appear at 9.4° and 23.8°, indicating an amorphous structure. This means that formaldehyde resin of melamine is formed from the methylol monomers and propagation of the polymeric backbone takes place. Figure 5 , it can be seen that the smaller peak from the two peaks of the MF resin t slightly overlaps the characteristic smectite peak at 8.1° [84,90]. This left-shifted and enlarged smectite peak is clearly shows that polymer molecules are intercalated in the interlayer space of the clay and nanocomposite is formed. The HRTEM image in Figure 2b also supports this claim.

The XRD pattern of the MF-organo clay-pumice composite (MFCPHC) in Figure 5 shows a peak with a wider and shorter peak height at 23.2°, reflecting the amorphous structure of pumice and possibly overlapping the peak of MF.In addition, the smectite peak, which appears to be shifted more to the left at 7.2° in the same pattern, indicates further intercalation of polymer chains in the interlayer space [79,86].

From the XRD pattern of the MF-organo clay-pumice-gypsum hybrid composite (MFCPGHC) in Figure 5, dihydrate calcium sulfate (at14.6 and 25.8°) and Bassanite (at 47.9,49.5 and 50.5°) and calcite (36.3°) as the main mineral phase with certain proportions of anhydrite crystals can be seen [91,92]. Also, the same pattern includes overlapping pumice and MF peaks and a smectite peak at 6.5°, showing almost exfoliation of the organo-clay layers. These findings are in line with the HRTEM image showing that relatively regular gypsum plates are heterogeneously dispersed next to pumice plates with a vitreous structure in which different phases are present as well as the clay platelets are exfoliated in the MF matrix [93,94].

The XRD pattern of the MF-organo clay-kaolin hybrid composite (MFCPKHC) in Figure 5e shows well-defined and characteristic peaks of kaolin at 12.2 °and 26.9°. On the other hand, it can be seen from this pattern that the MF and pumice peaks are overlapped and the smectite peak is shifted more to the left, which indicates that the organo-clay platelets are well exfoliated in the polymer matrix. Also, peaks corresponding to 30-36° and 39.1° reflect other mineral components of kaolin. Thus, it can be said that pumice plates, spherical polymer clay nanocomposites and kaolin plates can exhibit effective mixing due to interfacial compatibility (see Figure 2e and 3e) [89,95].

The XRD pattern of the MF-organo clay-pumice-hollow glass-sphere hybrid composite (MFCPHHC) in Figure 5 shows the overlapping MF, pumice and amorphous silica peaks and the smectite peak almost disappeared. Thus, as expected, the pumice plates and hollow glass spheres encapsulated by spherical polymer clay nanocomposites exhibited an ordered and relatively discrete arrangement (see Figure 2f and 3f) [82,90,96].

3.5. Thermal conductivities of raw montmorillonite (MMT), organo-montmorillonite (OMMT), melamine formaldehyde resin (MF), melamine formaldehyde orgono-clay nanocomposite (MFCNC) and various hybrid composites

Thermal conductivity is an important indicator for evaluating the thermal performance of a material under stationary conditions. The thermal conductivity coefficients measured for different samples were taken into account to evaluate the thermal insulation performances of the materials [97]. In this study, melamine formaldehyde resin and its nano-composite prepared using organo-clay were used as the main matrix and binder. While pumice was used as the main filling material, various hybrid composites were prepared by adding secondary fillers such as gypsum, kaolin and hollow glass sphere in certain proportions in order to improve the mechanical properties of the particularly brittle and friable material. The thermal conductivity coefficients of pure melamine formaldehyde resin (MF), MF-organo-clay nanocomposite (MFCNC) and MF-organo-clay-pumice (MFCPHC) and hybrid composites such as MF-organo-clay-pumice-gypsum (MFCPGHC), MF-organo-clay-pumice -kaolin (MFCPKHC) and MF-organo-clay-pumice-hollow glass sphere (MFCPHHC) are shown in Figure 6. It can be seen from this figure that the lowest thermal conductivity coefficients were obtained in MF-organo clay nanocomposite (MFCNC) and MF-organo-clay-pumice-hollow glass

Preprints (www.preprints.org) | NOT PEER-REVIEWED | Posted: 7 September 2023 doi:10.20944/preprints202309.0423.v1

sphere hybrid composite (MFCPHHC), respectively. In contrast, higher thermal conductivity coefficients were observed in MF-organo-clay-pumice (MFCPHC), MF-organo-clay-pumice-kaolin (MFCPKHC) hybrid composite and pure melamine formaldehyde resin (MF) composite, respectively.

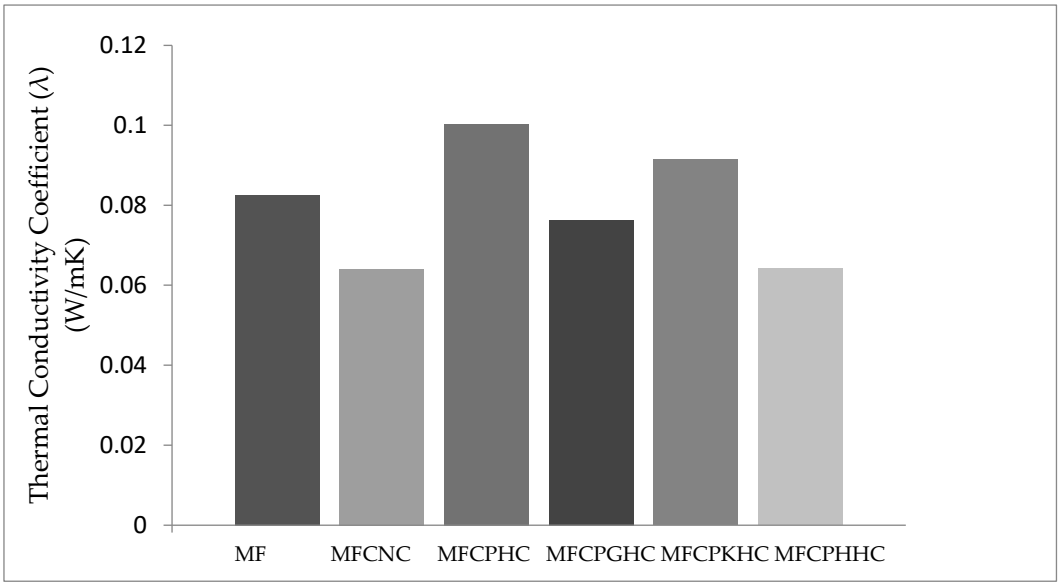

Figure 6. Analysis of thermal conductivities of pure melamine formaldehyde resin, MF-organo-clay nanocomposite and various hybrid composites.

The thermal conductivity of composites is anisotropic in nature and their correct design requires knowledge of the thermal conductivity of composites. Data on the thermal conductivity of resins facilitates the reduction of stresses caused by the shrinkage of the composites during curing and the mismatch in the coefficients of thermal expansion. Matrix materials can be of different types such as metal, mineral, ceramic and polymer. Polymer matrices, which can be thermoplastic or thermoset, are most widely used due to their cost efficiency, ease of manufacture, and also have excellent room temperature properties compared to other matrices [98]. Thermoset matrices are synthesized by the irreversible chemical reaction of a resin to an amorphous cross-linked polymer matrix. Due to their large molecular structure, thermoset resins provide good electrical and thermal insulation. Thermosets have a low viscosity, which allows for proper wetting of other additives, excellent thermal stability and better creep resistance. Thermoset resins can be formulated to give a wide variety of properties. Melamine formaldehyde resin hardens through the condensation reaction that produces water during the reaction and exhibits low shrinkage after curing, and has good chemical resistance and excellent mechanical properties. It also has excellent properties such as high temperature and creep resistance, good thermal insulation and sound damping properties, as well as superior flame retardancy properties [77,99].

The decrease in thermal conduction or the dominance of thermal insulation depend on the reduction of heat flow by limiting heat conduction, convection, radiation or all three. Thermal insulation materials can be categorized into three general types, which can be categorized as fibrous, cellular and granular. Fibrous insulations consist of small diameter fibers that finely divide the air space. The fibers may be perpendicular or parallel to the insulated surface and may or may not be bonded together. Silica, glass, rock wool, slag wool and alumina silica fibers are used. The most commonly used insulations of this type are fiberglass and mineral wool. Cellular insulations contain small individual cells separated from each other and glass or polystyrene (closed cell) and other polymeric foams are typical examples. Granular insulators have small nodules that contain voids or cavities, and they are not considered true cellular materials as there may be material transfer between the voids. Granular insulations such as calcium silicate, expanded vermiculite, perlite, pumice, gypsum, cellulose, diatomaceous earth and expanded polystyrene can be produced as a

Preprints (www.preprints.org) | NOT PEER-REVIEWED | Posted: 7 September 2023 doi:10.20944/preprints202309.0423.v1

loose or crumbly material but combined with a binder and fiber to form a rigid insulation material [100].

Thermal conductivity is strongly correlated with filler/polymer interface properties. The use of different fillers or chemical modification of fillers can be widely used to improve polymer/filler interface interactions [101]. Improved filler/matrix affinity can increase the effectiveness of interfacial attraction interactions and significantly reduce interfacial energy, as for nanocomposites with polymer and nano fillers [102].

In the thermoset melamine formaldehyde matrix, regular spherical clusters were formed during foaming due to the exfoliation of organo-clay platelets and the reduction of the solvent and polymer chain interface energy, resulting in a very high thermal insulation performance and a lower thermal conductivity coefficient (see Figures 2b and 3b).

In the composite, where the pumice plates exhibit a more regular and relatively uniform arrangement with the inclusion of hollow glass spheres encapsulated by spherical polymer clay nanocomposites, the negative effect of the presence of pumice in terms of thermal insulation was compensated by the hollow glass spheres and thus the second lowest thermal conductivity coefficient with the granular insulation types were obtained [103].

The gypsum-containing composite, in which the relatively regular gypsum boards are surrounded by heterogeneously dispersed and significantly deformed polymer clay nanocomposite spheres (see Figures 2d and 3d), next to the pumice boards with a vitreous structure, exhibited a relatively high thermal insulation performance. This can be explained by the fact that the deformed nanocomposite spheres inhibit the flow of heat through the fibril structures of the exfoliated organo-clay platelets [104].

Kaolin-containing composite, in which coarse-textured glassy pumice sheets, spherical polymer clay nanocomposite and kaolin sheets exhibited an effective blending, showed lower void ratio and higher thermal conductivity coefficient, and therefore lower thermal insulation performance, in parallel with its compact structure (see Figures 2e and 3e) [105].

3.6. Dependence of densities, flexural strengths, modulus of elasticity and screw holding strengths of hybrid composites on their composition

Figure 7 a, b, c and d shows the comparison of density, flexural strength, modulus of elasticity, and screw holding strength of hybrid composites such as MF-organo-clay-pumice (MFCPHC), MF-organo-clay-pumice-gypsum (MFCPGHC), MF-organo-clay-pumice-kaolin (MFCPKHC) and MF-organo-clay-pumice-hallow glass sphere (MFCPHHC).

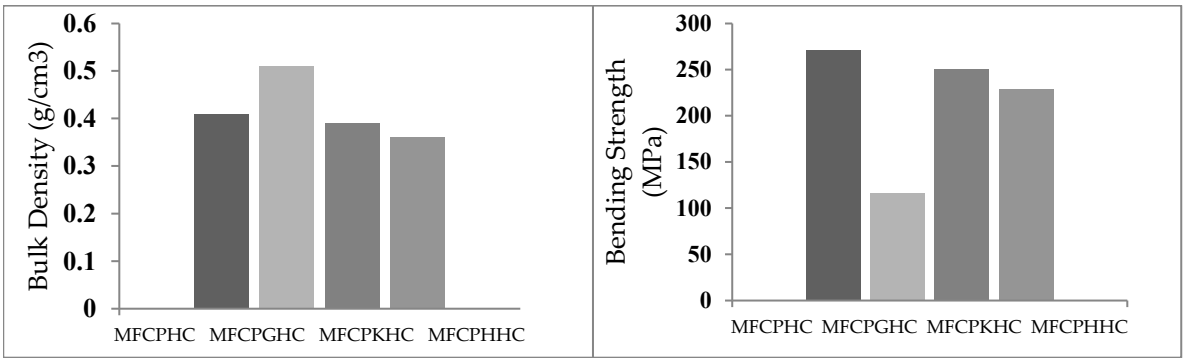

(**a**) (**b**)

Preprints (www.preprints.org) | NOT PEER-REVIEWED | Posted: 7 September 2023 doi:10.20944/preprints202309.0423.v1

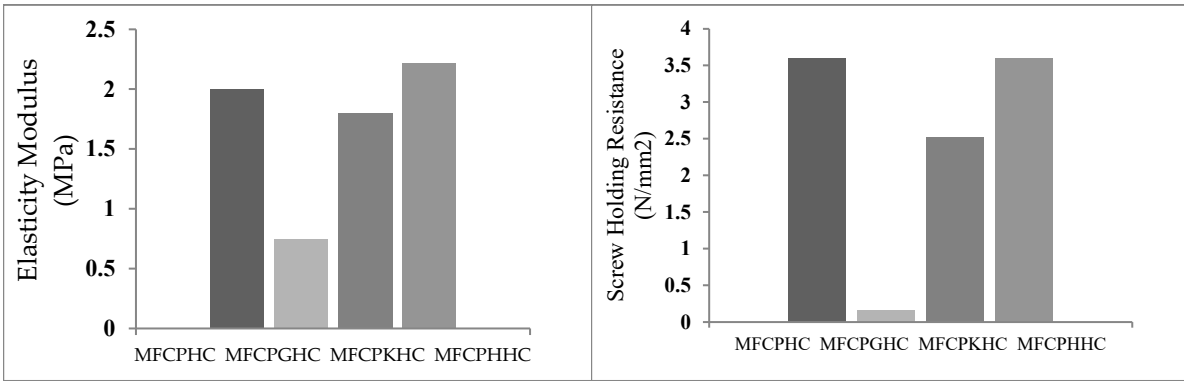

(c) (d)

Figure 7. Variation of densities (a), flexural strengths (b), modulus of elasticity(c) and screw holding strengths (d) of hybrid composites with their composition.

It can be seen from Figure 7a that the hybrid composites bulk densities follow the order of (MFCPHHC)<(MFCPKHC) <(MFCPHC) <(MFCPGHC). As expected, the lowest density was found in the composite containing hallow glass sphere, and the highest density was found in the composite containing gypsum. In the gypsum-containing composite, the deformation of the globular clusters of the organo-clay nano-composite resulted in a more rigid and compact structure, and thus a higher density. The composite containing the partially swelling kaolin by resin intercalation exhibited a slightly smaller density in parallel with the expanding volume. Density of composite bulk, besides being dependent on resin/composite content, is also determinant in mechanical properties such as flexural strength, modulus of elasticity and screw holding strength [106].

As can be seen from Figure 7b, the highest flexural strength of the four hybrid composites was observed in the sample containing only pumice, and the lowest strength was observed in the sample containing gypsum. With a relatively low density and a surface morphology indicating a highly effective inter granular interaction between coarse-textured glassy pumice plates, spherical polymer clay nanocomposites, and kaolin layers arranged in different directions but regularly, the kaolin-containing composite exhibited a very high flexural strength (see Figure 3) [107]. In contrast, the low-density composite containing relatively low impact strength-hollow glass spheres with a surface morphology created by clustered hollow glass spheres effectively surrounded by arranged layers of kaolin, pumice plates and spherical polymer clay nanocomposites has extremely high flexural strength. demonstrated, which may imply very efficient interface compatibility (see Figure 3) [108]. Low flexural strength of the gypsum-containing composite is an expected mechanical behavior due to its morphological structure, which indicates a structuring of polymer clay nanocomposite spheres in the voids and superficial folds or fractures of the porous pumice plates, and the presence of heterogeneous agglomerates (see Figures 2 and 3) [109].

From Figure 7c it can be seen that the modulus of elasticity of the composites follows the sequence MFCPHHC > MFCPHC > MFCPKHC > MFCPGHC. It can be seen from Figure 7d that the screw holding strengths also follow a similar sequence. From this close similarity, it can be concluded that composites containing only pumice and hollow glass sphere are ductile materials with high performance and high toughness [110].

On the other hand, when the thermal conductivity of composites containing only pumice and hollow glass sphere is compared, it can be seen from Figure 6 that the composite containing pumice has a value approximately twice as high as the composite containing hollow glass sphere. Thus, although the pumice-containing composite does not contain a highly porous structure, its high elasticity and screw holding resistance can be explained by the construction of a very stable network structure. Both the low modulus of elasticity and the very low screw holding resistance indicate that the gypsum-containing composite is a brittle material with an unstable textural structure [111].

Consequently, it can be argued that the composite containing a hollow glass sphere is the most suitable hybrid composite in terms of both thermal insulation and mechanical strength.

Acknowledgments: This study was supported by Atatürk University Scientific Research Projects Coordination Unit (BAP) (Project Code: FDK-2022-10258). The authors are grateful to Atatürk University for their financial support.

References

1. Alireza Kaboorani: B.R., Pierre Blanchet, Marco Fellin, Omid Hosseinaei, Sequin Wang, Nanocrystalline cellulose (NCC): A renewable nano-material for polyvinyl acetate (PVA) adhesive. European Polymer Journal, 2012. 48(11): p. 1829-1837.
2. M.F. Pour, H.K., A. Dorieh, M.V. Kiamahalleh, K.D. Hoseini, Utilization of phenol formaldehyde/Fe3O4 nanocomposite as microwave preheating amplifier in laminated veneer lumber (LVL) structure. Journal of Building Engineering, 2022. 46.
3. M.F. Pour, M.M., M.V. Kiamahalleh, K.D. Hoseini, H. Hatefnia, A. Dorieh, Biological durability of particleboard: fungicidal properties of Ag and Cu nanoparticles against Trametes versicolor white-rot fungus. Wood Material Science & Engineering, 2022. 17(6): p. 1-8.
4. B. Voigt, D.H.M., M. Pelišková, N. Rozhkova, Electrical and mechanical properties of melamine-formaldehyde–based laminates with shungite filler. POLYMER COMPOSITES, 2005.
5. Jeronimidis, W.G.G., Wood pulp fiber reinforced melamine-formaldehyde composites. Journal of Materials Science 2004. 39: p. 3245-3247.
6. P.-O. Hagstrand, K.O., Mechanical properties and morphology of flax fiber reinforced melamine-formaldehyde composites. Mechanical Properties and Morphology, 2001. 22(4).
7. S.M.M. Mousavi, E.A., M. Tajvidi, D.W. Bousfield, M. Dehghani-Firouzabadi, Application of cellulose nanofibril (CNF) as coating on paperboard at moderate solids content and high coating speed using blade coater. Progress in Organic Coatings, 2018. 122: p. 207-218.
8. P.K. Ghosh, K.K., and Arun Kumar, Studies on Thermal and Mechanical Properties of Epoxy-Silicon Oxide Hybrid Materials. Journal of Materials Engineering and Performance, 2015. 24: p. 4440-4448.
9. Hsieh, T.H.K., A. J.; Masania, K., Taylor, A. C.; Sprenger, S, the mechanisms and mechanics of the toughening of epoxy polymers modified with silica nanoparticles. Polymer, 2021. 51(26): p. 6284-6294.
10. Rouhani, M.R., A, Perlite–SO 3 H nanoparticles: very efficient and reusable catalyst for three-component synthesis of N-cyclohexyl-3-aryl-quinoxaline-2-amine derivatives under ultrasound irradiation. Journal of the Iranian Chemical Society, 2018. 15: p. 2375-2382.
11. Calebrese, C.H., L.; Schadler, L. S.; Nelson, J. K, A review on the importance of nanocomposite processing to enhance electrical insulation. IEEE Transactions on Dielectrics and Electrical Insulation, 2011. 18(4): p. 938-945.
12. Ramazani, A.R., M.; Joo, S. W., Silica nanoparticles from rice husk ash: a green catalyst for the one-pot three-component synthesis of benzo [B] furan derivatives. Advanced Materials Research, 2014. 875: p. 202-207.
13. Bittmann, B.H., F.; Schlarb, A. K., Ultrasonic dispersion of inorganic nanoparticles in epoxy resin. Ultrasonics Sonochemistry, 2009. 16: p. 622-628.
14. Johnsen, B.B.K., A. J.; Mohammed, R. D., Toughening mechanisms of nanoparticle-modified epoxy polymers. Polymer, 2007. 48(2): p. 530-541.
15. Giannelis, E.P., Polymer layered silicate nanocomposites. Advanced Materials, 1996. 8(1): p. 29-35.
16. Pavlidou, S.P., C. D., A review on polymer–layered silicate nanocomposites. Progress in Polymer Science, 2008. 33(12): p. 1119-1198.
17. Pol, M.H.L., G.; Zamani, E.; Ordys, A., Investigation of the ballistic impact behavior of 2D woven glass/epoxy/nanoclay nanocomposites. Journal of Composite Materials, 2015. 49(12): p. 1449-1460.
18. Pol, M.H.L., G. H., Studies on the mechanical properties of composites reinforced with nanoparticles. Polymer Composites, 2017. 38(1): p. 205-212.
19. Fiedler, B.G., F. H.; Wichmann, M. H.; Nolte, M. C.; Schulte, K., Fundamental aspects of nano-reinforced composites. . Composites Science and Technology, 2006. 66(16): p. 3115-3125.
20. A. R. Annappa, S.B., J. Paulo Davim, Effect of organoclays on mechanical properties of glass fiber-reinforced epoxy nanocomposite. Polymer Bulletin, 2022. 79: p. 5085-5103.
21. Zhao, Q.B., S., The mechanism of filler action and the criterion of filler selection for reducing wear. Wear, 1999. 225-229(1): p. 660-668.
22. Karbhari, V.M., Non-Destructive Evaluation (NDE) of Polymer Matrix Composites. 2013, Elsevier.
23. Agubra, V.A.O., P. S.; Hosur, M. V., Influence of nanoclay dispersion methods on the mechanical behavior of E-glass/epoxy nanocomposites. Nanomaterials, 2013. 3(3): p. 550-563.
24. Nguyen, V.H.M.-C., S.; Carbonnier, B.; Di Tommaso, D.; Naili, S., From atomistic structure to thermodynamics and mechanical properties of epoxy/clay nanocomposites: Investigation by molecular dynamics simulations. Computational Materials Science, 2017. 139: p. 191-201.

25. Nguyen, V.H.M.-C., S.; Carbonnier, B.; Naili, S., Estimation of effective elastic properties of polymer/clay nanocomposites: A parametric study. Composites Part B: Engineering, 2018. 152: p. 139-150.
26. Vijayan, P.P.P., D.; Pionteck, J.; Kenny, J. M.; Thomas, S., Liquid-rubber-modified epoxy/clay nanocomposites: effect of dispersion methods on morphology and ultimate properties. Polymer Bulletin, 2015. 72: p. 1703-1722.
27. Wang, M.F., X.; Thitsartarn, W.; He, C., Rheological and mechanical properties of epoxy/clay nanocomposites with enhanced tensile and fracture toughnesses Polymer, 2015. 58: p. 43-52.
28. Chen, J.L.-R., A.; Trevarthen, J.; Gizewski, T.; Lukawski, D.; Hazra, K.; Rahatekar, S., S.; Koziol, K. K., Carbon nanotube films spun from a gas phase reactor for manufacturing carbon nanotube film/carbon fibre epoxy hybrid composites for electrical applications. Carbon, 2020. 158: p. 282-290.
29. Nayak, S.K.M., S.; Nayak, S. K., Thermal, electrical and mechanical properties of expanded graphite and micro-SiC filled hybrid epoxy composite for electronic packaging applications. Journal of ELECTRONIC MATERIALS, 2020. 49(1): p. 212-225.
30. Suresha, B.D., G. S.; Hemanth, G.; Somashekar, H. M., Physico-mechanical properties of nano silica-filled epoxy-based mono and hybrid composites for structural applications. Silicon, 2021. 13(7): p. 2319-2335.
31. Alsaadi, M., & Erkliğ, A., Effects of clay and silica nanoparticles on the Charpy impact resistance of a carbon/aramid fiber reinforced epoxy composite. Journal Materials Testing, 2019. 61(1): p. 65-70.
32. Toorchi, D.T., E.; Khosravi, H., Enhanced flexural and tribological properties of basalt fiber-epoxy composite using nano-zirconia/graphene oxide hybrid system. Journal of Indusrtrial Textiles, 2022. 51(2S): p. 238S–3252S.
33. Yashas Gowda, T.G.S., M. R.; Subrahmanya Bhat, K.; Madhu, P.; Senthamaraikannan, P.; Yogesha, B., Polymer matrix-natural fiber composites: An overview. Cogent Engineering, 2018. 5(1): p. 1-13.
34. Dogan, A.A., V., Low-velocity impact response of E-glass reinforced thermoset and thermoplastic based sandwich composites. Composites Part B: Engineering, 2017. 127: p. 63-69.
35. Mazumdar, S., Composites manufacturing: materials, product, and process engineering. CRC Press, 2001: p. 416 page.
36. Acikbas, G.Y., B., Wear response of glass fiber and ceramic tile-reinforced hybrid epoxy matrix composites Iranian Polymer Journal, 2019. 28: p. 21-29.
37. Rudresh, B.M., Ravi Kumar, B.N., Madhu, D., Combined effect of micro- and nano-fillers on mechanical, thermal, and morphological behavior of glass–carbon PA66/PTFE hybrid nano-composites. Advanced Composites and Hybrid Materials, 2019. 2: p. 176-188.
38. Rudresh, B.M.R.K., B. N.; Lingesh, B. V., Fibridization effect on the mechanical behavior of PA66/PTFE blend based fibrous composites. Transactions of the Indian Institute of Metals 2017. 70(10): p. 2683-2694.
39. Rudresh, B.M.R.K., B. N.; Lingesh, B. V., Hybridization Effect on the Mechanical Behavior of Monophase Reinforced PA66/Teflon Blend Based Hybrid Thermoplastic Composites. Transactions of the Indian Institute of Metals, 2017. 70(9): p. 2335–2346.
40. Osman, A.F.A., A. M.; Kalo, H.; Azmi, W. N. W.; Hashim, F., In vitro biostability and biocompatibility of ethyl vinyl acetate (EVA) nanocomposites for biomedical applications. RSC Advances, 2015. 5(40): p. 31485-31495.
41. Tolonen, H.S., S. G., Effect of mineral fillers on properties of composite matrix material. Mechanics of Composite Materials, 1996. 31(4): p. 317-324.
42. Shojaei, A.K., S. S., Self-healing and self-sensing smart polymer composites. Composite Materials, 2021: p. 307-357.
43. Murtaja, Y.L., L.; Sepetcioglu, H.; Vlček, J.; Lapčíková, B.; Ovsík, M.; Staněk, M., Enhancement of the mechanical properties of HDPE mineral nanocomposites by filler particles modulation of the matrix plastic/elastic behavior. journal Nanotechnology Reviews, 2022. 11: p. 312-320.
44. Usuki, A.K., Y.; Kawasumi, M.; Okada, A.; Fukushima, Y.; Kurauchi, T.; Kamigaito, O., Synthesis of nylon 6-clay hybrid. Journal of Materials Research, 1993. 8(5): p. 1179-1184.
45. Adesakin, A.O.A., O. O.; Imosili, P. E.; Attahdaniel, B. E.; Olusunle, S. O. O., Characterization and Evaluation of Mechanical Properties of Dolomite as Filler in Polyester. Chemistry and Materials Research, 2013. 3(8).
46. Chong, L.K.O., A. F.; Fauzi, A. A. A.; Alrashdi, A. A.; Halim, K. A. A., The Mechanical and Thermal Properties of Poly (ethylene-co-vinyl acetate) (PECoVA) Composites with Pristine Dolomite and Organophilic Microcrystalline Dolomite (OMCD). Polymers, 2021. 13(18): p. 2-27.
47. Osman, A.F.S., L.; Alrashdi, A. A.; Ul-Hamid, A.; Ibrahim, I., Improving the tensile and tear properties of thermoplastic starch/dolomite biocomposite film through sonication process. Polymers, 2021. 13: p. 274.
48. Morreale, M.L., A.; Mistretta, M. C.; Ascione, L.; La Mantia, F. P., Mechanical, Thermomechanical and Reprocessing Behavior of Green Composites from Biodegradable Polymer and Wood Flour. Materials, 2015. 8(11): p. 7536-7548.
49. Hsissou, R.S., R.; Benzekri, Z.; Hilali, M.; Rafik, M.; Elharfi, A., Polymer composite materials: A comprehensive review. Composite Structures, 2021. 262.

50. Alakrach, A.M., Osman, A. F., Noriman, N. Z., Betar, B. O., & Dahham, O. S., Thermal properties of ethyl vinyl acetate (EVA)/montmorillonite (MMT) nanocomposites for biomedical applications. MATEC Web of Conferences, 2016. 78.
51. Hamid, A.R.A.O., A. F.; Mustafa, Z.; Mandal, S.; Ananthakrishnan, R., Tensile, fatigue and thermomechanical properties of poly (ethylene-co-vinyl acetate) nanocomposites incorporating low and high loadings of pre-swelled organically modified montmorillonite. Polymer Testing, 2020. 85.
52. Osman, A.F.F., T. F. M.; Rakibuddin, M.; Hashim, F.; Johari, S. A. T. T.; Ananthakrishnan, R.; Ramli, R., Pre-dispersed organo-montmorillonite (organo-MMT) nanofiller: Morphology, cytocompatibility and impact on flexibility, toughness and biostability of biomedical ethyl vinyl acetate (EVA) copolymer. Materials Science and Engineering: C, 2017. 74: p. 194-206.
53. Sun, T., Fan, H., Wang, Z., Liu, X., & Wu, Z., Modified nano Fe2O3-epoxy composite with enhanced mechanical properties. Materials & Design, 2015. 87: p. 10-16.
54. Bal, S., Experimental study of mechanical and electrical properties of carbon nanofiber/epoxy composites. Materials & Design 2010. 31(5): p. 2406-2413.
55. Radoman, T.S., Džunuzović, J. V., Jeremić, K. B., Grgur, B. N., Miličević, D. S., Popović, I. G., & Džunuzović, E. S. Materials & Design, Improvement of epoxy resin properties by incorporation of TiO2 nanoparticles surface modified with gallic acid esters. Materials & Design, 2014. 62: p. 158-167.
56. Becker, C., Krug, H., & Schmidt, H., Tailoring of thermomechanical properties of thermoplastic nanocomposites by surface modification of nanoscale silica particles. Materials Research Society, 1996. 435: p. 237.
57. Carotenuto, G., Her, Y. S., & Matijević, E., Preparation and characterization of nanocomposite thin films for optical devices. Industrial & engineering chemistry research, 1996. 35(9): p. 2929-2932.
58. Rong, M.Z., Zhang, M. Q., Liu, H., Zeng, H., Wetzel, B., & Friedrich, K., Microstructure and tribological behavior of polymeric nanocomposites. Industrial Lubrication and Tribology, 2001. 53(2): p. 72-77.
59. Kumar, A., Anant, R., Kumar, K., Chauhan, S. S., Kumar, S., & Kumar, R., Anticorrosive and electromagnetic shielding response of a graphene/TiO 2–epoxy nanocomposite with enhanced mechanical properties. RSC Advances, 2016. 6.
60. Xia, H., & Wang, Q., Preparation of conductive polyaniline/nanosilica particle composites through ultrasonic irradiation. Journal of Applied Polymer Science, 2003. 87: p. 1811-1817.
61. Xu, L.R., Bhamidipati, V., Zhong, W., H.,Li, J., Lukehart, C.,M., Mechanical Property Characterization of a Polymeric Nanocomposite Reinforced by Graphitic Nanofibers with Reactive Linkers. Journal of Composite Materials, 2004. 38(18): p. 1563-1582.
62. Gürses, A., Güneş, K., Mindivan, F., Korucu, M. E., Açıkyıldız, M., & Doğar, Ç., The investigation of electrokinetic behaviour of micro-particles produced by CTA+ ions and Na-montmorillonite. Applied Surface Science, 2014. 318: p. 79-84.
63. Singla, P., Mehta, R., & Upadhyay, S. N., Clay modification by the use of organic cations. Green and sustainable chemistry, 2012. 2(1): p. 22-25.
64. Santos, E.C.D., Bandeira, R. M., Vega, M. L., & Santos Junior, J. R. D., Poly (melamine-formaldehyde-silica) composite hydrogel for methylene blue removal. Materials Research 2021. 24(4).
65. Zhu, P., Gu, Z., Hong, S., & Lian, H., Preparation and characterization of microencapsulated LDHs with melamine-formaldehyde resin and its flame retardant application in epoxy resin. Polymers for Advanced Technologies, 2018. 29(7): p. 2147-2160.
66. Vaia, R.A., & Giannelis, E. P., Lattice model of polymer melt intercalation in organically-modified layered silicates. Macromolecules. Macromolecules, 1997. 30(25): p. 7990–7999.
67. GÜNİSTER CANBAZ, E., Synthesis and characterization of biopolymer/clay nanocomposites, in INSTITUTE OF NATURAL SCIENCES. 2008, ISTANBUL TECHNICAL UNIVERSITY.
68. International, A.S.T.M., ASTM 1037 16, in Standard Test Method for Evaluating Properties of Wood-Base Fiber and Particle Panel Materials. 2007, Annual book of ASTM standards.
69. International, A.S.T.M., ASTM D790, in Standard test methods for flexural properties of unreinforced and reinforced plastics and electrical insulating materials. 2007, Annual book of ASTM standards.
70. Naresh, R., Parameshwaran, R., & Ram, V. V., Microcapsules of n-dodecanoic acid/melamine-formaldehyde with enhanced thermal energy storage capability for solar applications. Journal of Science: Advanced Materials and Devices, 2022. 7(3).
71. Gürses, A., & Barın, T. B., Preparation, Structural Characterization and Evaluation of Some Dynamic and Rheological Properties of a New Type of Clay Containing Mastic Material, Clay-Mastic. Minerals, 2023. 13(705): p. 2-16.
72. Gürses, A., Güneş, K., Şahin, E., & Açıkyıldız, M., Investigation of the removal kinetics, thermodynamics and adsorption mechanism of anionic textile dye, Remazol Red RB, with powder pumice, a sustainable adsorbent from waste water. Frontiers in Chemistry, 2023. 11: p. 14.

73. Jia, C., Zhu, G., Legg, B. A., Guan, B., & De Yoreo, J. J., Bassanite Grows Along Distinct Coexisting Pathways and Provides a Low Energy Interface for Gypsum Nucleation. Crystal Growth & Design, 2022. 22(11): p. 6582-6587.
74. Hong, H., Churchman, G. J., Gu, Y., Yin, K., & Wang, C., Kaolinite–smectite mixed-layer clays in the Jiujiang red soils and their climate significance. Geoderma, 2012. 173-174: p. 75-83.
75. Luo, M., Liu, Y., Hu, J., Li, J., Liu, J., & Richards, R. M., General strategy for one-pot synthesis of metal sulfide hollow spheres with enhanced photocatalytic activity. Applied Catalysis B: Environmental, 2012. 125: p. 180-188.
76. Gao, Y., Liu, S., Wang, Q., & Wang, G., Preparation of melamine–formaldehyde resin grafted by (3-aminopropyl) triethoxysilane for high-performance hydrophobic materials. Journal of Applied Polymer Science, 2020: p. 10.
77. Nemanič, V., Zajec, B., Žumer, M., Figar, N., Kavšek, M., & Mihelič, I., Synthesis and characterization of melamine–formaldehyde rigid foams for vacuum thermal insulation. Applied Energy, 2014. 114: p. 320-326.
78. Razaghi, K.M., Hasankhani, H., & Koukabi, M., Improvement in physical and mechanical properties of butyl rubber with montmorillonite organo-clay. Iranian Polymer Journal, 2007. 16(10): p. 671-679.
79. Sever, K., Atagür, M., Tunçalp, M., Altay, L., Seki, Y., & Sarıkanat, M., The effect of pumice powder on mechanical and thermal properties of polypropylene. Journal of Thermoplastic Composite Materials, 2019. 32(8): p. 1092-1106.
80. Erbs, A., Nagalli, A., de Carvalho, K. Q., Mymrin, V., Passig, F. H., & Mazer, W., Properties of recycled gypsum from gypsum plasterboards and commercial gypsum throughout recycling cycles. Journal of Cleaner Production, 2018. 183: p. 1314-1322.
81. Sarma, G.K., Sen Gupta, S., & Bhattacharyya, K. G., Removal of hazardous basic dyes from aqueous solution by adsorption onto kaolinite and acid-treated kaolinite: kinetics, isotherm and mechanistic study. SN Applied Sciences 2019. 1(211): p. 15.
82. Zhang, W., Zhangsun, X., & Tao, Y., Photocatalytic degradation of Red 2G on the suspended TiO 2-hollow glass sphere. Reaction Kinetics, Mechanisms and Catalysis, 2021. 134: p. 569–578.
83. Chen, Z., Wang, J., Yu, F., Zhang, Z., & Gao, X. (2015)., Preparation and properties of graphene oxide-modified poly (melamine-formaldehyde) microcapsules containing phase change material n-dodecanol for thermal energy storage. Journal of Materials Chemistry A, 2015. 3: p. 11624–11630.
84. Gürses, A., Doğar, Ç., Köktepe, S., Mindivan, F., Güneş, K., & Aktürk, S., Investigation of Thermal Properties of PUF/colored Organoclay Nanocomposites. ACTA PHYSICA POLONICA A, 2015. 127(4): p. 979-983.
85. Wanyika, H., Maina, E., Gachanja, A. and Marika, D., Instrumental characterization of montmorillonite clays by X-ray fluorescence spectroscopy, fourier transform infrared spectroscopy, X-ray diffraction and uv/visible spectrophotometry. Journal of Agriculture, Science and Technology, 2016. 17(1): p. 224-239.
86. Khorzughy, S.H., Eslamkish, T., Ardejani, F. D., & Heydartaemeh, M. R., Cadmium removal from aqueous solutions by pumice and nano-pumice. Korean Journal of Chemical Engineering, 2015. 32: p. 88-96.
87. Ahmed, A., Chaker, Y., Belarbi, E. H., Abbas, O., Chotard, J. N., Abassi, H. B., Nguyen Van Nhien,A., El Hadri, M., ... & Bresson, S. , XRD and ATR/FTIR investigations of various montmorillonite clays modified by monocationic and dicationic imidazolium ionic liquids. Journal of Molecular Structure, 2018. 1173: p. 653-664.
88. Kumar, A., & Lingfa, P., Sodium bentonite and kaolin clays: Comparative study on their FT-IR, XRF, and XRD. Materials Today: Proceedings, 2020. 22(3): p. 737-742.
89. Tironi, A., Trezza, M. A., Irassar, E. F., & Scian, A. N., Thermal treatment of kaolin: effect on the pozzolanic activity. Procedia Materials Science, 2012. 1: p. 343-350.
90. Yu, C., Xu, W., Zhao, X., Xu, J., & Jiang, M., Effects of the reaction degree of melamine-formaldehyde resin on the structures and properties of melamine-formaldehyde/polyvinyl alcohol composite fiber. Fibers and Polymers, 2014. 15(9): p. 1828-1834.
91. Hossain, M.S., & Ahmed, S., Synthesis of nano-crystallite gypsum and bassanite from waste Pila globosa shells: crystallographic characterization. RSC Advances, 2022. 12: p. 25096–25105.
92. Sakae, T., Sato, Y., Numata, Y., Suwa, T., Hayakawa, T., Suzuki, K., Kuwada, T, Hayakawa, K., Hayakawa, Y., Tanaka, T., & Sato, I., Thermal ablation of FEL irradiation using gypsum as an indicator. Lasers in Medical Science 2007. 22: p. 15-20.
93. Guler, U.A., & Sarioglu, M., Removal of tetracycline from wastewater using pumice stone: equilibrium, kinetic and thermodynamic studies. JOURNAL OF ENVIRONMENTAL HEALTH SCIENCE & ENGINEERING, 2014.
94. Sepehr, M.N., Amrane, A., Karimaian, K. A., Zarrabi, M., & Ghaffari, H. R., Potential of waste pumice and surface modified pumice for hexavalent chromium removal: characterization, equilibrium, thermodynamic and kinetic study. Journal of the Taiwan Institute of Chemical Engineers, 2014. 45(2): p. 635-647.

95. Gardolinski, J.E.F.C., & Lagaly, G., Grafted organic derivatives of kaolinite: II. Intercalation of primary n-alkylamines and delamination. Clay Minerals, 2005. 40(4).
96. Schwinger, L., Lehmann, S., Zielbauer, L., Scharfe, B., & Gerdes, T., Aluminum Coated Micro Glass Spheres to Increase the Infrared Reflectance. Coatings, 2019. 9(187): p. 2-20.
97. Amaral, C., Vicente, R., Ferreira, V. M., & Silva, T., Polyurethane foams with microencapsulated phase change material: Comparative analysis of thermal conductivity characterization approaches. Energy and Buildings, 2017. 153: p. 392-402.
98. Frontini, P., M. and Pouzada, A., S., Chapter 6 - Trends in the multifunctional performance of polyolefin/clay nanocomposite injection moldings. Multifunctionality of Polymer Composites, 2015: p. 213-244.
99. Wang, X., Li, C., & Zhao, T., Fabrication and characterization of poly (melamine- formaldehyde)/silicon carbide hybrid microencapsulated phase change materials with enhanced thermal conductivity and light-heat performance. Solar Energy Materials and Solar Cells, 2018. 1836: p. 82-91.
100. Șova, D., Domnica Stanciu, M. and Georgescu, S., V., Design of Thermal Insulation Materials with Different Geometries of Channels. Polymers (Basel), 2021. 13: p. 2-14.
101. Ma, H., Gao, B., Wang, M., Yuan, Z., Shen, J., Zhao, J., & Feng, Y., Strategies for enhancing thermal conductivity of polymer-based thermal interface materials: A review. Journal of Materials Science 2021. 56: p. 1064–1086
102. Almuallim, B., Harun, W. S. W., Al Rikabi, I. J., & Mohammed, H. A., Thermally conductive polymer nanocomposites for filament-based additive manufacturing. Journal of Materials Science, 2022. 57: p. 3993-4019.
103. Uysal, H., Demirboğa, R., Şahin, R., & Gül, R., The effects of different cement dosages, slumps, and pumice aggregate ratios on the thermal conductivity and density of concrete Cement and Concrete Research, 2004. 34(5): p. 845-848.
104. Romero-Gómez, M.I., Silva, R. V., Costa-Pereira, M. F., & Flores-Colen, I., Thermal and mechanical performance of gypsum composites with waste cellulose acetate fibres. Construction and Building Materials, 2022. 356.
105. Michot, A., Smith, D. S., Degot, S., & Gault, C., Thermal conductivity and specific heat of kaolinite: Evolution with thermal treatment. Journal of the European Ceramic Society, 2008. 28(14): p. 2639-2644.
106. Jorda J, K.G., Barbu MC, Petutschnigg A, Král P., Influence of Adhesive Systems on the Mechanical and Physical Properties of Flax Fiber Reinforced Beech Plywood. Polymers (Basel). Polymers, 2021. 13.
107. Kwon, Y.M., Chang, I., & Cho, G. C., Consolidation and swelling behavior of kaolinite clay containing xanthan gum biopolymer. Acta Geotechnica, 2023. 18: p. 3555-3571.
108. Wang, H., Yan, R., Cheng, H., Zou, M., Wang, H., & Zheng, K., Hollow glass microspheres/phenolic syntactic foams with excellent mechanical and thermal insulate performance. . Frontiers in Chemistry, 2023: p. 10 pages.
109. He, W., Li, B., Meng, X., & Shen, Q., (2023). Compound Effects of Sodium Chloride and Gypsum on the Compressive Strength and Sulfate Resistance of Slag-Based Geopolymer Concrete. Buildings, 2023. 13(3): p. 3-25.
110. Hariyadi and Tamai, H., Enhancing the Performance of Porous Concrete by Utilizing the Pumice Aggregate. Procedia Engineering, 2015. 125: p. 732-738.
111. Huang, J.S., & Gibson, L. J., Elastic moduli of a composite of hollow spheres in a matrix. Journal of the Mechanics and Physics of Solids, 1993. 41(1): p. 55-75.